IOP Publishing Journal of Physics: Condensed Matter
J. Phys.: Condens. Matter **26** (2014) 436003 (7pp) doi:10.1088/0953-8984/26/43/436003

Anisotropy of magnetic properties of $Fe_{1+y}Te$

G E Grechnev[1], A S Panfilov[1], A V Fedorchenko[1], A A Lyogenkaya[1], I P Zhuravleva[1], D A Chareev[2,3], A N Nekrasov[2], E S Mitrofanova[4], O S Volkova[4,5], A N Vasiliev[4,5,6] and O Eriksson[7]

[1] B Verkin Institute for Low Temperature Physics and Engineering, National Academy of Sciences of Ukraine, 61103 Kharkov, Ukraine
[2] Institute of Experimental Mineralogy, Russian Academy of Sciences, Chernogolovka, Moscow Region 142432, Russia
[3] National Research University Higher School of Economics, 20 Myasnitskaya Ulitsa, Moscow 101000, Russia
[4] Low Temperature Physics and Superconductivity Department, Physics Faculty, Moscow State University, Moscow 119991, Russia
[5] Theoretical Physics and Applied Mathematics Department, Institute of Physics and Technology, Ural Federal University, 620002 Yekaterinburg, Russia
[6] National University of Science and Technology 'MISiS', Moscow 119049, Russia
[7] Division of Materials Theory, Department of Physics and Astronomy, Uppsala University, Box 516, SE-75120, Sweden

E-mail: grechnev@ilt.kharkov.ua

Received 21 July 2014, revised 4 September 2014
Accepted for publication 10 September 2014
Published 9 October 2014

Abstract

The magnetic properties of $Fe_{1+y}Te$ single crystals ($y \simeq 0.1 \div 0.18$) were studied at temperatures $4.2 \div 300$ K. At an ambient pressure, with decreasing temperature a drastic drop in $\chi(T)$ was confirmed at $T \simeq 60 \div 65$ K, which appears to be closely related to the antiferromagnetic (AFM) ordering. It is found that the magnitudes of the anisotropy of magnetic susceptibility $\Delta\chi$ in the AFM phase are close in the studied samples, whereas the sign of the anisotropy apparently depends on the small variations of the excess iron y in $Fe_{1+y}Te$ samples. The performed DFT calculations of the electronic structure and magnetic properties for the stoichiometric FeTe compound indicate the presence of frustrated AFM ground states. There are very close energies and magnetic moments for the double stripe configurations, with the AFM axes oriented either on the basal plane or along the [0 0 1] direction. Presumably, both these configurations can be realized in $Fe_{1+y}Te$ single crystals, depending on the variations of the excess iron. This can provide different signs of magnetic anisotropy in the AFM phase, presently observed in the $Fe_{1+y}Te$ samples. For these types of AFM configuration, the calculations for the FeTe values of $\Delta\chi$ are consistent with our experimental data.

Keywords: Fe-based superconductors, magnetic anisotropy, magnetic susceptibility, FeTe, electronic structure

(Some figures may appear in colour only in the online journal)

1. Introduction

The novel superconducting $FeSe_{1-x}Te_x$ compounds have received extensive attention due to the simplest crystal structure among the new families of the iron-based layered systems exhibiting superconductivity [1–7]. This structural simplicity favours the experimental and theoretical studies of chemical substitution and high pressure effects, which are aimed at promoting a better understanding of the mechanism of the superconductivity and also at tuning the properties of

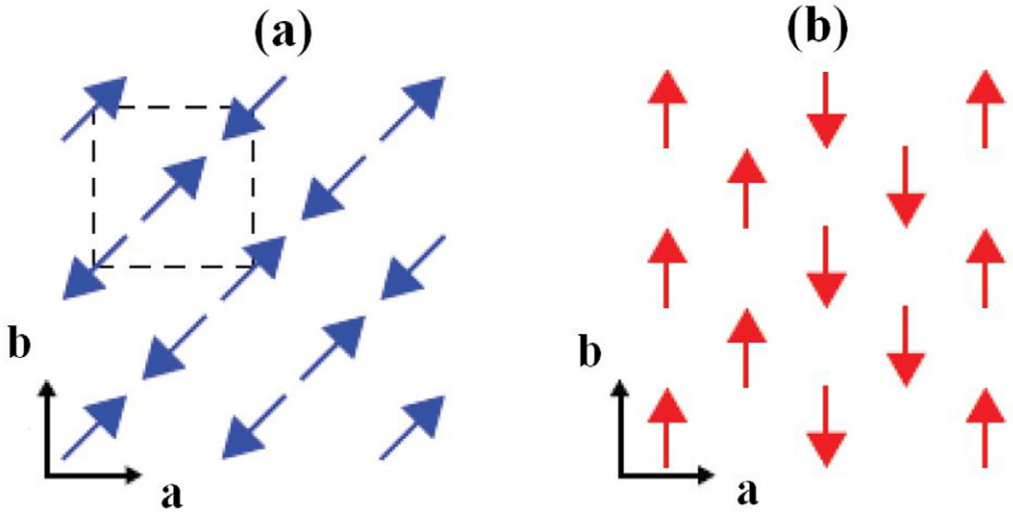

Figure 1. The arrangements of Fe magnetic moments on the basal plane for possible AFM orderings in FeTe: (*a*) single stripes (SS); (*b*) double stripes (DS).

the novel superconducting materials. It is presently believed that the superconductivity in the FeSe(Te) system originates from several coupled degrees of freedom, such as the magnetic, charge and elastic ones [3].

The superconducting properties of $FeSe_{1-x}Te_x$ are characterized by the non-monotonic dependence of transition temperatures T_c on composition. A noticeable increase in T_c with x was found, from ~8 K at $x = 0$ to a maximum value of ~15 K at $x \simeq 0.5$, with a subsequent fall to 0 K near $x \sim 0.9$ [3]. Both the FeSe and FeTe compounds have similar electronic structures and Fermi surface (FS) nestings, which might be favorable for the unconventional superconductivity mediated by the spin fluctuations at the nesting vector of the spin density wave [8]. In Fe–As-based superconductors, such fluctuations correspond to a 'single-stripe' (SS) antiferromagnetic (AFM) pattern with the (π, π) ordering vector, which was observed in the corresponding parent Fe–As compounds. There were theoretical predictions that FeTe could also be a superconductor due to the similar FS nesting [8–10]. However, the bulk $Fe_{1+y}Te$ compounds display an ambient pressure below $T \simeq 70$ K an AFM ground state with the unique so-called 'double-stripe' (DS) ordering and the $(\pi, 0)$ propagation vector [11–14] (see figure 1).

A drastic drop in the temperature dependence of the magnetic susceptibility $\chi(T)$ was observed with a decreasing temperature at $T \simeq 70$ K [15, 16]. This peculiarity is related to a first-order structural phase transition accompanied by the onset of AFM ordering [4, 11, 12]. Below the phase transition the crystal structure depends on the amount of excess iron y in $Fe_{1+y}Te$ systems, which possess the same tetragonal crystal structure at room temperature. For nearly stoichiometric $Fe_{1+y}Te$ compounds, at low temperatures a monoclinic structure and a commensurate in-ab-plane AFM ordering were observed [4, 12]. The origin of the strong correlation between the structural and magnetic transitions in $Fe_{1+y}Te$ is not yet clear. It has been argued [11] that the main contribution to the entropy change at the transition(s) can be provided by AFM ordering. This favors the view that the transition is driven by magnetism. An opposite conclusion was, however, put forward in [2, 4].

On the assumption that the suppression of the structural and magnetic transitions stimulates the onset of superconductivity, attempts have been made to find the superconductivity in FeTe by applying high pressure [9, 17]. However, no trace of superconductivity was detected at pressures up to 190 kbar in the electrical resistivity measurements, whereas a puzzling increase in magnetization with pressure was observed [17]. Recently, the *negative* pressure effect on the superconducting transition temperature was observed in tellurium-rich $FeSe_{1-x}Te_x$ compounds at $x \sim 0.8-0.9$ [18]. In fact, the superconductivity was detected at about 13 K in FeTe by applying tensile stress conditions in the thin films of the compound [19], which involve an in-plane extension and an out-of-plane contraction of the lattice. Also, the strong positive pressure effect on the magnetic susceptibility was revealed for both the paramagnetic and AFM phases of FeTe [16]. Finally, it was recently established [20, 21] that FeTe transforms from a low pressure AFM phase to a ferromagnetic (FM) phase at pressures above 2 GPa.

It appears that the magnetism in FeTe cannot be explained by the spin density wave instability due to the (π, π) FS nesting, which is similar to the nesting in other iron-based superconductors [8]. It was suggested [13, 14, 22] that the observed DS magnetic ordering in FeTe can be mediated by local spin moment interactions, also including a contribution of itinerant electrons, but not in line with the FS nesting scheme. In [23] it was shown that the doping of FeTe with excess iron can provide a novel FS nesting in $Fe_{1+y}Te$, which could explain the DS AFM $(\pi, 0)$ ordering. However, this effect has not been confirmed by the ARPES studies [24].

Taken together, these experimental and theoretical findings indicate that the electronic and magnetic properties of $Fe_{1+y}Te$ compounds are closely correlated with the crystal structure parameters and the amount of excess iron. Further studies are needed to explore the mechanisms of magnetism in FeTe and to elucidate the origin of its magnetic and structural

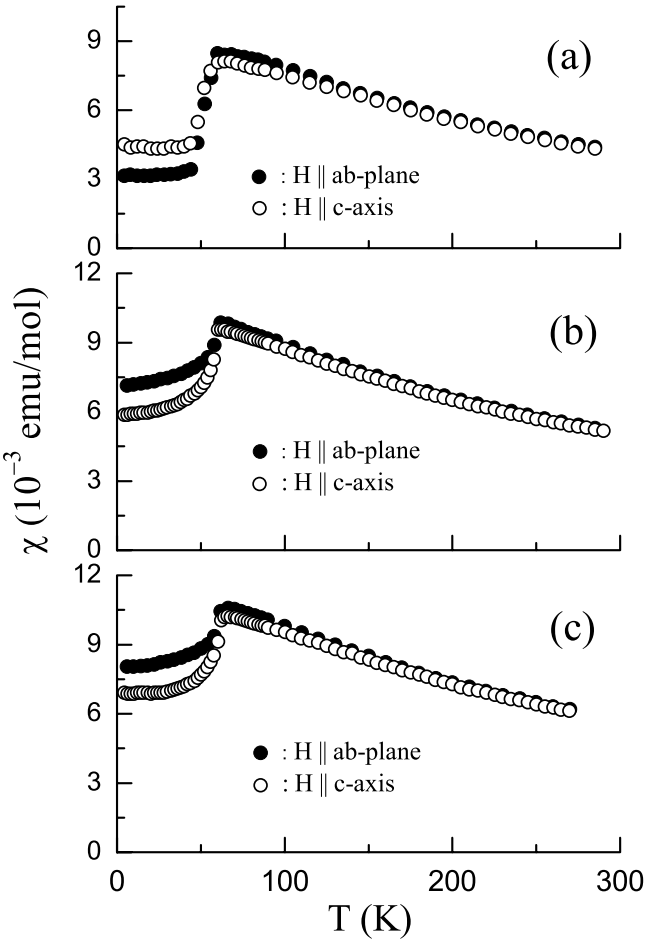

Figure 2. The temperature dependence of the magnetic susceptibility for the FeTe single crystals #3422 (*a*), #3599 (*b*) and #3271 (*c*).

transitions. In this work we present the results of experimental and theoretical studies of the anisotropy of magnetization for $Fe_{1+y}Te$ single crystals at low temperatures. The first-principles calculations of the electronic structure and magnetic properties of FeTe are carried out to shed light on the observed magnetic anisotropy for the AFM phase.

2. Experimental details and results

The single crystals of the $Fe_{1+y}Te$ compound were grown using a recrystallization-in-halides-flux technique under a constant temperature gradient, which is the driving force of the recrystallization process (for details, see [7, 25]). The mixture of the Fe and Te powders was dissolved in molten salts in the hot end of a quartz ampoule and transferred to its cold end, where crystallization occured. The difference between the upper and lower temperatures in the ampoule was about 50–100 K. The sample #3271 was synthesized in KCl/NaCl eutectic flux at an upper temperature of about 790 °C. The other samples, #3422 and #3599, were synthesized in CsCl/NaCl/KCl flux and the temperatures at the hot end of the ampoules were kept at 750 °C and 710 °C, respectively. In all cases, the duration of the synthesis was about 30 days. The typical dimensions of the produced plate-like single crystals

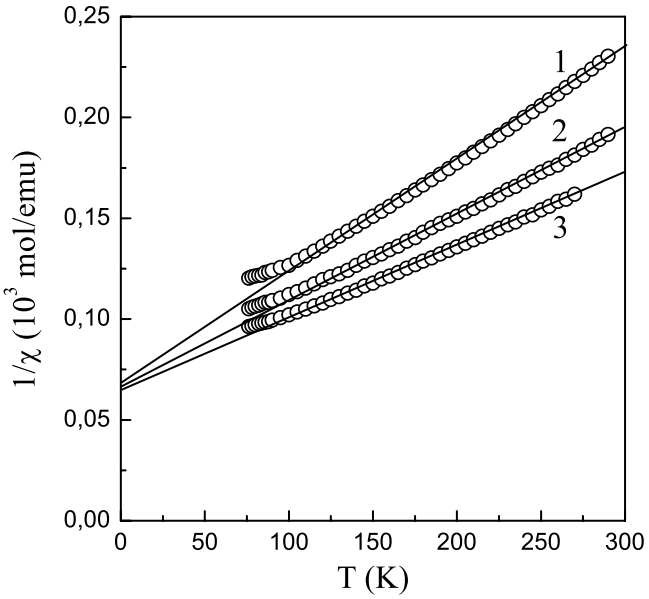

Figure 3. The temperature dependencies of the inverse magnetic susceptibility in the $H \parallel ab$-plane for the FeTe samples #3422 (1), #3599 (2) and #3271 (3) together with their straight-line fit.

were $(1 \div 3) \times (1 \div 3) \times (0.2 \div 0.3)\,\mathrm{mm}^3$. Their tetragonal $P4/nmm$ structure was confirmed at room temperature by an x-ray diffraction technique. The chemical composition of the samples was studied with a digital scanning electron microscope TESCAN Vega II XMU with the energy dispersive micro analysis system INCA Energy 450. As an external standard, the iron telluride $FeTe_2$ was chosen, which had been prepared in a similar way to the abovementioned method and possessed the exact stoichiometric phase with a narrow homogeneity region [26]. In this case, the accuracy of the determined components ratio was not worse than 2%.

The dc magnetic susceptibility was measured at $T = 4 \div 300$ K using a superconducting quantum interference device (SQUID) magnetometer with a magnetic field $H = 500$ Oe which was applied both along the *c*-axis and in the *ab*-plane. As shown in figure 2, the temperature dependencies of the magnetic susceptibility $\chi(T)$ for all the samples exhibit an anomaly at $T = 60 \div 65$ K, which is in agreement with the literature data. At temperatures above this anomaly the samples are in the paramagnetic state and for $T \geqslant 100$ K their observed $\chi(T)$ behaviour is approximately described by the Curie–Weiss (CW) law:

$$\chi(T) \simeq C/(T - \Theta). \qquad (1)$$

The corresponding values of the CW parameters, resulted from the best straight-line fit of the inverse magnetic susceptibility for the $Fe_{1+y}Te$ compounds, as shown in figure 3, are listed in table 1. The observed large and negative values of Θ indicate dominant AFM interactions and appear to be linearly dependent on the square of the effective magnetic moment, $\Theta \propto \mu_{\mathrm{eff}}^2$.

The puzzling peculiarity of the $Fe_{1+y}Te$ compounds in the AFM state is the observed change in sign of the magnetic anisotropy, $\Delta\chi = \chi_{\parallel c} - \chi_{\perp c}$, with an increase in the

Table 1. Curie–Weiss parameters, paramagnetic Curie temperature Θ (in unit of K), Curie constant C (K·emu/mole) and effective magnetic moment $\mu_{\rm eff}$ ($\mu_{\rm B}$/atom Fe) and value of magnetic anisotropy, $\Delta\chi = \chi_{\parallel c} - \chi_{\perp c}$ at $T = 0$ K (10^{-3} emu/mole), for studied $Fe_{1+y}Te$ samples with different Fe content.

Sample	1+y	Θ	C	$\mu_{\rm eff}$	$\Delta\chi$
#3422	1.13 ± 0.02	-123	1.59	3.6	1.26 ± 0.05
#3599	1.15 ± 0.02	-155	2.00	4.0	-1.27 ± 0.05
#3271	1.18 ± 0.02	-177	2.33	4.3	-1.15 ± 0.05

excess Fe (see figure 2 and table 1), which is reported here for the first time. Moreover, the magnitude of $\Delta\chi$ at $T = 0$ K remains nearly the same for all the studied samples. This behaviour of the anisotropy implies that the direction of the AFM axis changes from being along the ab-plane to the c-crystallographic direction. Furthermore, one might assume that these states with a different magnetic structure can be almost degenerate. To verify this assumption, we have further calculated and compared the ground state energies, corresponding to these two types of magnetic structure in FeTe.

In addition, we would like to touch on the question of $Fe_{1+y}Te$ magnetic anisotropy in the basal plane for the AFM structure with the magnetic moments lying in the ab-plane. For a perfect and single-domain crystal, one can reasonably expect the magnetic anisotropy to be close in magnitude to that given in table 1. However, as follows from the detailed structural analysis, our single crystals have a block structure. This could probably explain a much smaller experimentally observed in-plane anisotropy, which is presumably related to the lack of the single-domain state.

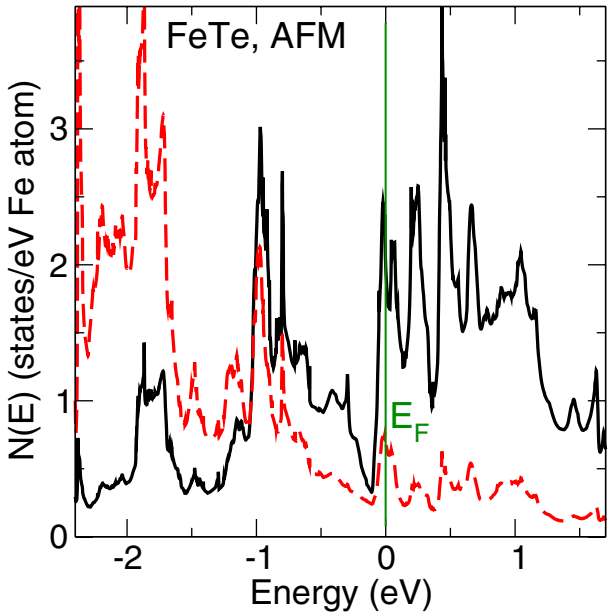

Figure 4. Calculated spin-majority (dashed line) and spin-minority (solid line) densities of electronic states per Fe atom for the DS AFM ordered FeTe. The position of the Fermi level at $E = 0$ is marked by a vertical line.

3. Details and results of electronic structure calculations

In the present work, we attempted to investigate the peculiarities of AFM ordering in the $Fe_{1+y}Te$ compounds, including the anisotropy of the AFM magnetic susceptibility and the relative energies of different DS AFM configurations. For this purpose, the electronic structure of the DS AFM state of the stoichiometric FeTe compound was calculated within the density functional theory (DFT) by using the relativistic LMTO method with a full potential (FP-LMTO, RSPt implementation [27–30]) and the linearized augmented plane waves method with a full potential (FP-LAPW, Elk implementation [31]). The exchange and correlation potentials were treated within the local spin density approximation (LSDA [32]) and the generalized gradient approximation (GGA [33]) of the DFT. For the employed full potential FP-LMTO and FP-LAPW methods no restrictions were imposed on the charge densities or potentials of the studied systems, which is especially important for the anisotropic layered structure of FeTe.

At temperatures above 70 K the $Fe_{1+y}Te$ compounds possess a tetragonal PbO-type crystal structure (space group $P4/nmm$), which exhibits strong two-dimensional features. The positions of the Te sheets are fixed by the internal parameter Z, which represents the height of the chalcogen atoms above the iron square plane and determines the Te–Fe bond angles. The $Fe_{1+y}Te$ systems with $y \leqslant 0.1$ exhibit a first-order phase transition near 70 K with a small monoclinic distortion of the crystal lattice, which is accompanied by the DS AFM ordering [4, 11, 12]. The corresponding crystal structure parameters of $Fe_{1+y}Te$ compounds were established in a number of works by means of x-ray and neutron diffraction studies [3–5, 11] and we used these experimental data in our calculations.

In agreement with the previously reported calculations of [13, 34–37] the DS AFM phase of FeTe is found to be the ground state. The calculated spin-split densities of the states in the DS AFM ordered state of FeTe are presented in figure 4.

In order to gain insight into the experimentally observed magnetic anisotropy of the $Fe_{1+y}Te$ samples, the total energies and magnetic moments of the DS AFM state of FeTe were calculated for the [1 0 0], [0 1 0] and [0 0 1] AFM axes of magnetization. For this purpose we considered the $[2a \times b \times c]$ magnetic cell. The structural parameters a, b and c were taken according to [4, 11], whereas the angle between the a and c axes was taken as 90° (instead of 89.2° in the weakly monoclinic distorted structure). All the relativistic effects, including the spin–orbit coupling, were incorporated to reveal the magnetic anisotropy of FeTe. To estimate the anisotropy of magnetic susceptibilities $\Delta\chi$ for the DS ordered AFM state

Table 2. The calculated relative total energies ΔE (meV/f.u.), the magnetic moments M (μ_B/atom Fe) and the anisotropy of magnetic susceptibility, $\Delta\chi = \chi_{\parallel c} - \chi_{\perp c}$ (10^{-3} emu/mole), of the AFM DS FeTe for the AFM axes of magnetization taken along [1 0 0], [0 1 0] and [0 0 1] directions.

	ΔE				M				$\Delta\chi$
	RSPt		Elk		RSPt		Elk		Elk
AFM axis	LSDA	GGA	LSDA	GGA	LSDA	GGA	LSDA	GGA	GGA
[1 0 0]	+0.4	+0.6	+0.4	+0.9	2.16	2.37	2.23	2.51	1.19
[0 1 0]	+0.3	+0.4	+0.2	+0.6	2.16	2.37	2.23	2.51	1.20
[0 0 1]	0	0	0	0	2.16	2.37	2.23	2.51	−1.24

of FeTe, the self-consistent calculations of the field-induced magnetic moments were carried out with the FP-LAPW Elk code [31] for the [1 0 0], [0 1 0] and [0 0 1] AFM magnetization axes. The directions of the external field **H** were taken both along and perpendicular to the c axis. The resulted values of the relative total energies, magnetic moments and the anisotropy of the magnetic susceptibility of FeTe, $\Delta\chi = \chi_{\parallel c} - \chi_{\perp c}$ are presented in table 2.

4. Discussion

The calculated value of the DOS at the Fermi level $N(E_F) \simeq 3$ states/eV per f.u. for the DS AFM phase can be compared with experimental data on the electronic specific heat coefficient in FeTe, $\gamma_{exp} \simeq 34$ mJ mol^{-1} K^{-2} [15, 38]:

$$\gamma_{exp} = (1 + \lambda)\gamma_{theor}, \qquad (2)$$

The corresponding renormalization parameter λ includes the electron–phonon (λ_{el-ph}) and spin-fluctuation (λ_{sf}) contributions and, according to equation (2), amounts to $\lambda \simeq 3.8$. It should be noted, that the contribution of the spin-fluctuations λ_{sf} can be rather large for the itinerant systems close to magnetic instability [28]. The reduction of the superconducting transition temperature for $FeSe_{1-x}Te_x$ compounds in the vicinity of the end member FeTe indicates that these strong spin fluctuations presumably do not support superconductivity, but rather can prevent the onset of superconductivity in FeTe [18].

As can be seen in table 2, the evaluated ground state energy in the DS AFM FeTe shows a weak preference for the AFM axes along the [0 0 1] direction. This result appeared to be valid for both the LSDA and GGA approximations, which were employed within two different DFT calculation methods, RSPt [29] and Elk [31]. However, the associated total energy gain is very small and all these magnetic configurations can be regarded as close-lying frustrated AFM states within about 1 meV of each other. This means that depending on the excess iron in the $Fe_{1+y}Te$ samples, the AFM axis of magnetization might be either within the ab-plane or along the c direction. Therefore the possibility of the AFM axis 'switching' can explain the experimentally observed different signs of the anisotropy of magnetic susceptibility in the AFM ordered single crystalline $Fe_{1+y}Te$ samples.

The calculated magnetic moments at the Fe sites of the DS AFM phase of FeTe are listed in table 2. It is found that, as compared with the LSDA results, the GGA gives larger values of magnetic moments for both the FP-LMTO and the FP-LAPW calculations. Basically, the calculated magnetic moments are in agreement with the results of neutron diffraction experiments ($M = 2.26 \div 2.54\,\mu_B$ [4, 11]). However, in every particular case the calculated value of M appeared to be independent of the direction of the magnetization, which could be related to the degeneracy of the AFM states with different magnetization axes.

The results of the field-induced calculations of the anisotropy of the magnetic susceptibility in table 2 are in a good agreement with the experimental data ($\Delta\chi_{exp} = 1.15 \div 1.27 \times 10^{-3}$ emu/mole, see table 1 and figure 2). The sign of the experimentally observed $\Delta\chi$ indicates that for the $Fe_{1+y}Te$ samples (b) and (c) in figure 2 the moments form the AFM structure with the spin directions along the c-axis. This provides some indication that a higher amount of excess iron, estimated as about $y \simeq 0.15$, can make the c-axis orientation of the spins in $Fe_{1+y}Te$ energetically favorable. On the other hand, a smaller amount of excess iron presumably causes a change in the AFM axis of the magnetization from the c-axis to the basal ab-plane, as in the case of the sample (a) in figure 2. In this connection we should note that for the $Fe_{1.07}Te$ sample the large spin moment 2.0 μ_B/Fe was observed in [11] along the b-axis direction, with the projections of the moment 0.72 μ_B and 0.71 μ_B along the a and c axes, respectively. On the other hand, no components along the a and c axis were detected in the $Fe_{1.05}Te$ single crystal [4], whereas a complicated incommensurate magnetic structure was reported for $Fe_{1.14}Te$ in [12].

The earlier established first-order structural/magnetic phase transition in $Fe_{1+y}Te$ [4, 11] also appears in figure 2(a), where $\chi(T)$ decreases abruptly at $T \sim 65$ K. However, for the investigated iron-enriched $Fe_{1+y}Te$ samples one can see a cusp at this temperature, as shown in figures 2(b) and (c), clearly indicating AFM ordering along the c-axis, which is presumably not accompanied by a simultaneous structural transition. In addition, for all the studied $Fe_{1+y}Te$ samples, the $\chi(T)$ dependencies, which were observed in the paramagnetic state (see figure 3), appeared to be close to a Curie–Weiss-like behavior. The ratio of the evaluated values of the effective magnetic moment, as shown in table 1, to the ordered magnetic moment resulting from the neutron studies at low temperatures is estimated to be about 2. In accordance with the Rhodes–Wohlfarth criterion this indicates the itinerant nature of FeTe magnetism.

5. Conclusions

The experimental studies of magnetic properties of $Fe_{1+y}Te$ single crystals at an ambient pressure revealed that the anisotropy values of their magnetic susceptibility in the AFM phase appeared to be close in magnitude for the studied samples. However, the sign of $\Delta\chi$ is different and can be determined by specific details of the DS AFM transition due to the variance in the amount of excess iron y.

The calculated electronic structure and magnetic properties of FeTe indicate the presence of nearly degenerate DS AFM configurations with different directions of magnetic ordering, both in the basal ab-plane and along [0 0 1] axis. These frustrated DS AFM states have substantially lower energy than that of the paramagnetic, ferromagnetic and single-stripe AFM states, and the electronic structure of the DS AFM state is very different from that of the SS AFM and FM states.

One might expect that the frustrated DS AFM configurations can be realized in $Fe_{1+y}Te$ single crystals, depending, for example, on the variations in the excess iron. This can provide different signs of magnetic anisotropy in the AFM phase, which were observed in the studied $Fe_{1+y}Te$ samples. Our results indicate that the signs of anisotropy of magnetization in the $Fe_{1+y}Te$ single crystals is in fact related to the amount of excess iron y, which is correlated with the ordering of the spins either in the ab-plane or along the c-axis. This is implicitly supported by the results of the supercell calculations of [39], which state that the presence of magnetic moments on the excess Fe sites can affect the fine details of AFM ordering by means of the interaction of the randomly distributed local moments with the itinerant magnetic subsystem of the iron layers.

Finally, the calculated value of the magnetic anisotropy of the AFM state appears to be consistent with our experimental data. It should be emphasized that the observed anisotropy of χ for the $Fe_{1+y}Te$ compounds was explained in this work by employing the DFT calculations of the total energies and magnetic susceptibilities in the external magnetic field. Therefore the obtained description of the experimental data is based on the assumed itinerant nature of the magnetic properties of FeTe. This is rather encouraging, taking into account that the Heisenberg model ran into problems when it was employed to explain the DS AFM structure of FeTe and the corresponding spin-wave spectrum [11, 14, 40].

Acknowledgments

This work was supported in part by the Ministry of Education and Science of the Russian Federation within the framework of Increase Competitiveness Program of NUST 'MISiS' (# K2-2014-036), by the Russian Foundation for Basic Research projects 13-02-00174, 14-02-92693, 14-02-92002, by CRDF grant No. FSAX-14-60108-0 and by the grant-in-aid of Ministry of Education and Science of Russia MK-7138.2013.2. OE acknowledges support from the Swedish Research Council (VR), the KAW foundation, eSSENCE and the ERC (project 247062-ASD).

References

[1] Khasanov R *et al* 2009 *Phys. Rev.* B **80** 140511
[2] McQueen T M, Williams A J, Stephens P W, Tao J, Zhu Y, Ksenofontov V, Casper F, Felser C and Cava R J 2009 *Phys. Rev. Lett.* **103** 057002
[3] Mizuguchi Y and Takano Y 2010 *J. Phys. Soc. Japan* **79** 102001
[4] Martinelli A, Palenzona A, Tropeano M, Ferdeghini C, Putti M, Cimberle M R, Nguyen T D, Affronte M and Ritter C 2010 *Phys. Rev.* B **81** 094115
[5] Viennois R, Giannini E, van der Marel D and Černý R 2010 *J. Solid State Chem.* **183** 769
[6] Fedorchenko A V *et al* 2011 *Low Temp. Phys.* **37** 83
[7] Ovchenkov Y A, Chareev D A, Kozlyakova E S, Volkova O S and Vasiliev A N 2013 *Physica* C **489** 32
[8] Subedi A, Zhang L, Singh D J and Du M H 2008 *Phys. Rev.* B **78** 134514
[9] Mizuguchi Y, Tomioka F, Tsuda S, Yamaguchi T and Takano Y 2009 *Physica* C **469** 1027
[10] Li J, Huang G Q and Zhu X F 2013 *Physica* C **492** 152
[11] Li S *et al* 2009 *Phys. Rev.* B **79** 054503
[12] Bao W *et al* 2009 *Phys. Rev. Lett.* **102** 247001
[13] Ma F, Ji W, Hu J, Lu Z-Y and Xiang T 2009 *Phys. Rev. Lett.* **102** 177003
[14] Moon C-Y and Choi H J 2010 *Phys. Rev. Lett.* **104** 057003
[15] Chen G F, Chen Z G, Dong J, Hu W Z, Li G, Zhang X D, Zheng P, Luo J L and Wang N L 2009 *Phys. Rev.* B **79** 140509
[16] Fedorchenko A V, Grechnev G E, Desnenko V A, Panfilov A S, Gnatchenko S L, Tsurkan V, Deisenhofer J, Loidl A, Volkova O S and Vasiliev A N 2011 *J. Phys.: Condens. Matter* **23** 325701
[17] Okada H, Takahashi H, Mizuguchi Y, Takano Y and Takahashi H 2009 *J. Phys. Soc. Japan* **78** 083709
[18] Panfilov A S, Pashchenko V A, Grechnev G E, Desnenko V A, Fedorchenko A V, Bludov A N, Gnatchenko S L, Chareev D A, Mitrofanova E S and Vasiliev A N 2014 *Low. Temp. Phys.* **40** 615
[19] Han Y, Li W Y, Cao L X, Wang X Y, Xu B, Zhao B R, Guo Y Q and Yang J L 2010 *Phys. Rev. Lett.* **104** 017003
[20] Bendele M, Maisuradze A, Roessli B, Gvasaliya S N, Pomjakushina E, Weyeneth S, Conder K, Keller H and Khasanov R 2013 *Phys. Rev.* B **87** 060409
[21] Bendele M, Pomjakushina E, Conder K, Khasanov R and Keller H 2014 *J. Supercond. Novel Magn.* **27** 965
[22] Johannes M D and Mazin I I 2009 *Phys. Rev.* B **79** 220510
[23] Han M-J and Savrasov S Y 2009 *Phys. Rev. Lett.* **103** 067001
[24] Nakayama K *et al* 2010 *Phys. Rev. Lett.* **105** 197001
[25] Chareev D, Osadchii E, Kuzmicheva T, Lin J Y, Kuzmichev S, Volkova O and Vasiliev A 2013 *Cryst. Eng. Commum.* **15** 1989
[26] Okamoto H and Tanner L E 1990 *Bull. Alloy Phase Diagrams* **11** 371
[27] Grechnev G E, Ahuja R and Eriksson O 2003 *Phys. Rev.* B **68** 064414
[28] Grechnev G E 2009 *Low Temp. Phys.* **35** 638
[29] Wills J M, Alouani M, Andersson P, Delin A, Eriksson O and Grechnev A 2010 *Full-Potential Electronic Structure Method: Energy and Force Calculations with Density Functional and Dynamical Mean Field Theory* (Berlin: Springer)
[30] http://fplmto-rspt.org/
[31] http://elk.sourceforge.net/
[32] von Barth U and Hedin L 1972 *J. Phys. C: Solid State Phys.* **5** 1629

[33] Perdew J P, Burke K and Ernzerhof M 1996 *Phys. Rev. Lett.* **77** 3865
[34] Ding M-C, Lin H-Q and Zhang Y-Z 2013 *Phys. Rev.* B **87** 125129
[35] Ciechan A, Winiarski M J and Samsel-Czekała M 2014 *J. Phys.: Condens. Matter* **26** 025702
[36] Kumar J, Auluck S, Ahluwalia P K and Awana V P S 2012 *Supercond. Sci. Technol.* **25** 095002
[37] Monni M, Bernardini F, Profeta G and Massidda S 2013 *Phys. Rev.* B **87** 094516
[38] Bud'ko S L, Canfield P C, Sefat A S, Sales B C, McGuire M A and Mandrus D 2009 *Phys. Rev.* B **80** 134523
[39] Zhang L, Singh D J and Du M-H 2009 *Phys. Rev.* B **79** 012506
[40] Glasbrenner J K, Velev J P and Mazin I I 2014 *Phys. Rev.* B **89** 064509